Phase behavior of dipolar associating fluids from the SAFT-VR+D equation of state

Honggang Zhao, Yuanyuan Ding, and Clare McCabe[a)]
Department of Chemical Engineering, Vanderbilt University, Nashville, Tennessee 37235

(Received 9 April 2007; accepted 13 June 2007; published online 31 August 2007)

The statistical associating fluid theory for potentials of variable range plus dipole (SAFT-VR+D) is extended to study associating dipolar fluids. In the SAFT-VR+D approach dipolar interactions are taken into account through the use of the generalized mean spherical approximation to describe a reference fluid of dipolar square-well segments. This enables the effect of the dipolar interactions on the thermodynamics and structure of fluids to be explicitly described. Predictions for the thermodynamic properties and phase behavior of dipolar associating square-well monomers with one, two, and four association sites are considered and compared with new isothermal-isobaric and Gibbs ensemble Monte Carlo simulation data. The results show that the SAFT-VR+D equation provides a good description of the phase behavior of dipolar associating fluids. Additionally we have applied the new theoretical approach to study the vapor pressure and saturated liquid density of water. © *2007 American Institute of Physics*. [DOI: 10.1063/1.2756038]

I. INTRODUCTION

Fluids with anisotropic interactions, such as polar or hydrogen bonding interactions, are important not only to the traditional oil and chemical industries, but also in environmental and biological systems; water, for example, is essential to all known forms of life and is considered the universal solvent. An accurate description of the phase behavior and thermodynamic properties of polar and associating fluids is therefore relevant to a diverse range of fields and applications.

Conventional engineering equations of state such as cubic equations, which provide a good description of the phase behavior of simple molecules and their mixtures, cannot easily be used to predict the phase equilibrium of associating and/or polar components. For example, such models cannot be used to study both the vapor-liquid equilibrium (VLE) and liquid-liquid equilibrium of alcohol-hydrocarbon mixtures using a single set of interaction parameters,[1] as the parameters are very sensitive to the state conditions to which they are fitted. Increasingly both industrial and academic interests are moving to the development and application of more advanced thermodynamic models that explicitly account for the molecular level interactions and so more accurately describe the physical nature of complex fluid systems.

Perhaps the simplest approach to modeling polar and/or associating fluids is the cubic-plus-association (CPA) equation,[2] which combines the Soave-Redlich-Kwong cubic equation of state with Wertheim's first order thermodynamic perturbation theory to describe hydrogen-bonding interactions. The CPA equation has been successfully applied to study a wide range of systems, including the VLE of alcohol-water-aliphatic hydrocarbon ternary mixtures using interaction parameters determined from the binary mixtures.[3] However, to describe fluids such as acetone, which are both polar and associating, self-association is used to mimic the strong interactions within the fluid, since the theory does not explicitly account for polar effects.[4]

An alternative approach to modeling associating and/or polar components is to use a molecular-based equation of state, such as the associated perturbed anisotropic chain theory (APACT) developed by Ikonomou and Donohue.[5] APACT models pure fluids that associate through hydrogen bonding interactions and takes into account interactions due to dipole and/or quadrupole moments;[6] however, for systems involving multipolar associating components, such as ethanol+pentanol, an analytical solution cannot be determined and the chemical and material equilibria must be solved numerically. At a similar level of theory, the molecular-based statistical associating fluid theory (SAFT) proposed by Chapman *et al.*[7] also explicitly takes into account nonsphericity and association interactions. SAFT, based on Wertheim's thermodynamic perturbation theory (TPT),[8] has proven to be a powerful equation of state for modeling associating and nonassociating chain fluids and their mixtures. In the SAFT framework, the free energy is written as the sum of four separate contributions as follows:

$$\frac{A}{Nk_BT} = \frac{A^{\text{ideal}}}{Nk_BT} + \frac{A^{\text{mono}}}{Nk_BT} + \frac{A^{\text{chain}}}{Nk_BT} + \frac{A^{\text{assoc}}}{Nk_BT}, \tag{1}$$

where N is the number of molecules, k_B Boltzmann's constant, and T the temperature. A^{ideal} is the ideal free energy, A^{mono} the contribution to the free energy due to the monomer segments, A^{chain} the contribution due to the formation of bonds between monomer segments, and A^{assoc} is the contribution due to association. Hence, a SAFT fluid is a collection of monomers that can form covalent bonds; the monomers interact via repulsive and attractive (dispersion) forces, and, in some cases, association interactions. Many different versions on the original SAFT equations have been reported in

[a)]Author to whom correspondence should be addressed. Electronic mail: c.mccabe@vanderbilt.edu

the literature which essentially correspond to different choices for the reference or monomer fluid, and different theoretical approaches to the calculation of the monomer free energy and structure.[9] In particular, several versions of the SAFT equation of state have been specifically developed to model polar fluids. In these, the dipolar and/or quadrupolar interactions are generally incorporated through the addition of the corresponding terms to Eq. (1). For the dipolar term, both the μ expansion proposed by Gubbins and Gray[10] (which describes the interaction of dipolar hard sphere fluids using an angular pair correlation function), and the more rapidly converging Padé approximation of Stell *et al.*,[11] have been widely adopted. For example, Muller and Gubbins[12] applied the μ expansion to describe water as a hard, spherical, associating, dipolar fluid within Wertheim's TPT theory, achieving good agreement with simulation and experimental data; Kraska and Gubbins[13] later extended the Lennard-Jones-SAFT theory of Muller and Gubbins using the multipolar μ expansion for the dipolar-dipolar interaction to study the phase behavior of alcohols and water and their mixtures with *n*-alkanes. Similarly, based on Wertheim's TPT, Nezbeda and Weingerl[14] developed a molecular-based equation of state for water that considers the dipole interaction as a perturbation term and Liu *et al.*[15] presented a SAFT-like equation of state based on a dipolar Yukawa potential for polar and associating fluids. However, a common feature of these equations of state is to treat nonspherical dipolar molecules as spherical dipolar fluids. As a result, the orientation of the dipolar interaction and the possibility of multiple polar sites within a molecule cannot be taken into account.

In contrast, Jog *et al.*[16] developed a SAFT equation of state (EOS) for tangent hard sphere chains with dipoles on alternate segments. In this work, although the position of the dipole moment is considered, the hard sphere pair correlation function is used to describe the pair correlation function between nondipolar and dipolar hard spheres at contact, and so neglects the effect of the dipole and its orientation. Using the same approach to describe dipolar interactions, Tumakaka and Sadowski[17] have extended the perturbed-chain SAFT (PC-SAFT) EOS to describe mixtures of nondipolar and polar molecules and Dominik *et al.*[18] have modeled the phase equilibria and thermodynamic properties of ethers and esters using PC-SAFT with dipolar contributions due to Jog *et al.* and Sagger and Fischer;[19] the two approaches were found to yield similar results for the systems studied. More recently, Gross and Vrabec[20] have developed a contribution for dipolar interactions based on third order perturbation theory which uses simulation data for the vapor-liquid equilibria of the two-center Lennard-Jones plus point dipole fluid to determine the model constants. The proposed term has been incorporated into the PC-SAFT equation of state and has been shown to improve the description of pure component and mixture phase equilibria for dipolar fluids over the original PC-SAFT approach.

In previous work we developed the SAFT-VR+D equation to describe the phase behavior and thermodynamic properties of dipolar fluids[21] through a combination of the SAFT-VR approach and the generalized mean spherical approximation (GMSA). The SAFT-VR equation is a version of the SAFT approach that models dispersion interactions through a potential of variable range[22] and has been successfully used to describe the phase equilibria of a wide range of industrially important systems; for example, alkanes of low molecular weight to simple polymers,[22–24] and their binary mixtures,[25,26,29,30] perfluoroalkanes,[27] water,[31] refrigerant systems,[32] and carbon dioxide,[26,28,31–33] have all been studied. In the modification of the SAFT-VR approach proposed by the authors to accurately treat dipolar fluids (SAFT-VR +D), the position and orientation of the dipole moment are explicitly described and its effect on the structure of the fluid incorporated through the use of a dipolar square-well reference fluid. With the SAFT-VR+D equation an accurate description of the *PVT* and phase behavior of dipolar square-well monomer and chain fluids, in which one or more segments are dipolar, can be obtained. In the current work, we extend the SAFT-VR+D approach to model dipolar associating fluids. Constant *NPT* and Gibbs ensemble Monte Carlo simulations have been performed to test and validate the new equation for dipolar associating fluids with one, two, and four association sites.

The remainder of the paper is organized as follows: in Sec. II we present the SAFT-VR+D model and theory for dipolar associating fluids. In Sec. III, details of the molecular simulations performed are presented. Results for the phase behavior of pure dipolar associating fluids are presented and compared with simulation data in Sec. IV along with results from the application of the SAFT-VR+D approach to study the phase behavior of water. Finally, concluding remarks are made and future work discussed in Sec. V.

II. THEORY

In the SAFT-VR+D approach molecules are modeled as hard spheres of diameter σ that can interact through the combination of a dipole moment μ embedded in the center of the sphere, a square-well interaction to describe the dispersion interactions, and short-range attractive square-well sites to describe association interactions that mimic hydrogen bonding. Hence the pair potential for the dipolar associating fluids studied in this work is defined by

$$u(\mathbf{r}\boldsymbol{\omega}_1\boldsymbol{\omega}_2\Omega_1\Omega_2) = u^{\mathrm{SW}}(r;\sigma) + u^{\mathrm{dipole}}(\mathbf{r}\boldsymbol{\omega}_1\boldsymbol{\omega}_2) + \sum_a \sum_b u_{ab}^{\mathrm{HB}}(\mathbf{r}\Omega_1\Omega_2), \tag{2}$$

where $\mathbf{r}$ is the vector between the center of the two monomers $r=|\mathbf{r}|$, $\boldsymbol{\omega}_i=(\theta_i,\phi_i)$ the set of angles defining the orientation of the dipole in monomer i, and Ω_i the orientation of associating site i relative to vector r. $u^{\mathrm{SW}}(r;\sigma)$ and $u^{\mathrm{dipole}}(\mathbf{r}\boldsymbol{\omega}_1\boldsymbol{\omega}_2)$ represent the isotropic square-well and anisotropic dipolar interaction potentials, respectively, and are given by

$$u^{\mathrm{SW}}(r;\lambda) = \begin{cases} 1, & \sigma < r < \lambda\sigma \\ 0, & r > \lambda\sigma \\ \infty, & r < \sigma, \end{cases}$$

where λ defines the range of the attractive square well and

$$u^{\text{dipole}}(\mathbf{r}\boldsymbol{\omega}_1\boldsymbol{\omega}_2) = -\frac{\mu^2}{r^3}D(\mathbf{n}_1\mathbf{n}_2\hat{\mathbf{r}}), \tag{3}$$

where

$$D(\mathbf{n}_1\mathbf{n}_2\hat{\mathbf{r}}) = 3(\mathbf{n}_1\cdot\hat{\mathbf{r}})(\mathbf{n}_2\cdot\hat{\mathbf{r}}) - \mathbf{n}_1\cdot\mathbf{n}_2. \tag{4}$$

Here $\hat{\mathbf{r}}$ is the unit vector in the direction of $\mathbf{r}$ joining the center of the segments and $\mathbf{n}_i$ the unit vector parallel to the dipole moment of segment i. The quantity u_{ab}^{HB} in Eq. (2) represents the association potential and is modeled by an anisotropic short-ranged square well interaction, where a and b represent the interacting associating sites. As can be seen in Fig. 1(a) the association sites are situated at a distance r_d from the center of the sphere. Sites of type a can bond to sites of type b on different molecules with an attractive energy ε^{HB} when the two sites are closer than a distance r_c apart. Sites of the same kind do not interact with each other.

In the SAFT-VR+D approach for dipolar associating fluids the Helmholtz free energy A can be written as a sum of three separate contributions as follows:

$$\frac{A}{Nk_BT} = \frac{A^{\text{ideal}}}{Nk_BT} + \frac{A^{\text{mono}}}{Nk_BT} + \frac{A^{\text{assoc}}}{Nk_BT}. \tag{5}$$

We will summarize each contribution to the free energy in turn. Note we do not consider the chain term as the systems studied in this work are monomer fluids; however, the SAFT-VR+D approach is straightforwardly applied to associating chain fluids through the addition of the chain term given in earlier work[21] to Eq. (5).

A. Ideal contribution

The free energy of an ideal gas is given by

$$\frac{A^{\text{ideal}}}{Nk_BT} = \ln(\rho\Lambda^3) - 1, \tag{6}$$

where $\rho = N/V$ is the number density of molecules, V is the volume of the system, and Λ is the thermal de Broglie wavelength. Since the ideal term is treated separately, the remaining terms are residual free energies.

B. Monomer contribution

The contribution to the Helmholtz free energy due to the monomer segments is given by

$$\frac{A^{\text{mono}}}{Nk_BT} = a^M, \tag{7}$$

where a^M is the excess Helmholtz free energy per dipolar square well monomer segment. Within the GMSA,[34] a^M is given by

$$a^M = a^{\text{dipole}} + a^{\text{isotropic}}, \tag{8}$$

where a^{dipole} is the contribution of the free energy due to the anisotropic dipolar interactions and the isotropic term $a^{\text{isotropic}}$ is given within the perturbation theory of Barker and Henderson[35] by

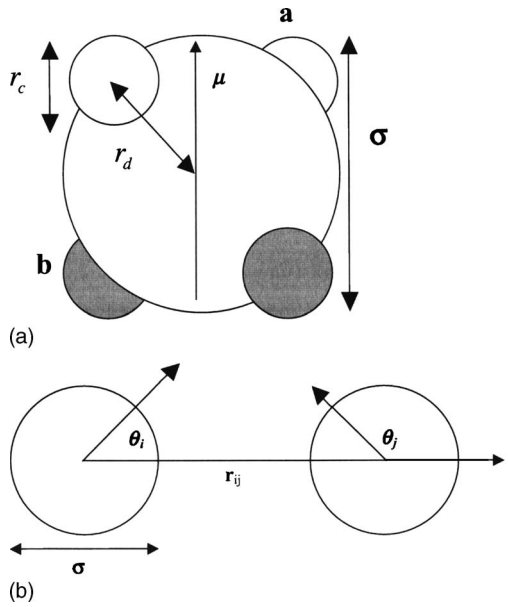

FIG. 1. Schematic illustrating the SAFT-VR+D dipolar associating fluid model and the interaction potential used in the (a) SAFT-VR+D approach and (b) the MC simulations.

$$a^{\text{isotropic}} = a^{\text{HS}} + \beta a_1^{\text{SW}} + \beta^2 a_2^{\text{SW}}, \tag{9}$$

where $\beta = 1/k_BT$ and a^{HS} is obtained from the Carnahan and Starling[36] equation

$$a^{\text{HS}} = \frac{4\eta - 3\eta^2}{(1-\eta)^2} \tag{10}$$

and

$$\eta = (\pi/6)\rho_s\sigma^3. \tag{11}$$

As in the original SAFT-VR approach, using the mean-value theorem, the first perturbation term[37] a_1^{SW} can be obtained as

$$a_1^{\text{SW}} = -4\eta\varepsilon(\lambda^3 - 1)g^{\text{HS}}(1;\eta_{\text{eff}}), \tag{12}$$

where $g^{\text{HS}}(1;\eta_{\text{eff}})$ can be evaluated using the Carnahan and Starling equation;

$$g^{\text{HS}}(1;\eta_{\text{eff}}) = \frac{1 - \eta_{\text{eff}}/2}{(1-\eta_{\text{eff}})^3}. \tag{13}$$

Here, η_{eff} is the effective packing fraction that in the range $1.1 \leqslant \lambda \leqslant 1.8$ is given by

$$\eta_{\text{eff}}(\eta,\lambda) = c_1\eta + c_2\eta^2 + c_3\eta^3, \tag{14}$$

with coefficients

$$\begin{pmatrix} c_1 \\ c_2 \\ c_3 \end{pmatrix} = \begin{pmatrix} 2.258\,55 & 0.249\,434 & 0.249\,434 \\ -0.669\,270 & -0.827\,739 & -0.827\,739 \\ 10.157\,6 & 5.308\,27 & 5.308\,27 \end{pmatrix} \times \begin{pmatrix} 1 \\ \lambda \\ \lambda^2 \end{pmatrix}. \tag{15}$$

The second perturbation term a_2^{SW} is obtained from the first density derivative of a_1^{SW} within the local compressibility approximation

TABLE I. Model parameters for dipolar associating fluids studied. μ^{*2} is the reduced dipole moment defined by $\mu^{*2}=\mu^2/(4\pi\varepsilon_0 k_B\varepsilon\sigma^3)$ where $\varepsilon_0=8.85\times10^{-12}$, λ the range of the potential, ε^* the reduced depth of square-well potential, r_{12}^* the reduced cutoff radius for the association interactions, and ε^{HB*} the reduced association energy.

System	Sites	μ^{*2}	λ	r_{12}^*	ε^*	ε^{HB*}
1	1	1.0	1.5	1.05	1	5
2	2	1.0	1.5	1.05	1	5
3	4	1.0	1.5	1.05	1	2
4	4	1.0	1.5	1.05	1	5
5	4	1.0	1.5	1.05	1	7
6	4	1.0	1.5	1.1	1	5
7	4	1.0	1.5	1.1	1	3
8	4	0.5	1.5	1.05	1	5
9	4	2.0	1.5	1.05	1	5

$$a_2^{SW}=\frac{1}{2}\varepsilon K^{HS}\eta\frac{\partial a_1^{SW}}{\partial\eta}, \tag{16}$$

where K^{HS} is the hard-sphere isothermal compressibility of Percus and Yevick[38] (PY),

$$K^{HS}=\frac{(1-\eta)^4}{1+4\eta+4\eta^2}. \tag{17}$$

From Wertheim's solution of the Ornstein-Zernike equation for dipolar hard spheres with the MSA closure,[39] the excess free energy due to the dipolar interactions is obtained as

$$a^{dipole}=-\frac{8}{\eta}\xi^2\left[\frac{(1+\xi)^2}{(1-2\xi)^4}+\frac{(2-\xi)^2}{8(1+\xi)^4}\right]. \tag{18}$$

Here $\xi=\kappa\eta$, where κ is a scaling parameter determined from

$$3y=q_{PY}(\kappa\eta)-q_{PY}(-\kappa\eta), \tag{19}$$

with $q_{PY}(\eta)$ the dimensionless inverse compressibility of Percus and Yevick[39] given by

$$q_{PY}(\eta)=\frac{(1+2\eta)^2}{(1-\eta)^4} \tag{20}$$

and y the strength of the dipolar effect[39]

$$y=\frac{4\pi}{9}\rho\beta\mu^2. \tag{21}$$

C. Association contribution

Based on the theory of Wertheim, the contribution due to association for s sites on a molecule is obtained as[40]

TABLE II. *NPT* MC simulation results for systems 1 and 2. The reduced temperature is given by $T^*=k_BT/\varepsilon$, the reduced pressure is given by $P^*=P\sigma^3/\varepsilon$, and the reduced energy is given by $E^*=E/N\varepsilon$.

System	T^*	P^*	η	*Error*	$-E^*$	*Error*	System	T^*	P^*	η	*Error*	$-E^*$	*Error*
1	1.2	0.1003	0.315	±0.011	5.42	±0.19	2	1.2	0.0262	0.346	±0.012	7.66	±0.31
		0.6731	0.360	±0.008	6.13	±0.14			0.5231	0.378	±0.008	8.38	±0.25
		2.0315	0.401	±0.006	6.80	±0.12			1.7509	0.415	±0.006	9.24	±0.23
		4.7581	0.449	±0.005	7.48	±0.10			4.2774	0.456	±0.005	10.12	±0.21
	1.4	0.5651	0.310	±0.010	5.16	±0.18		1.4	0.5113	0.328	±0.010	6.46	±0.25
		1.3937	0.358	±0.007	5.95	±0.14			1.2845	0.368	±0.008	7.30	±0.23
		3.1441	0.403	±0.005	6.65	±0.10			2.9360	0.410	±0.006	8.19	±0.21
		6.4672	0.450	±0.005	7.31	±0.10			6.0980	0.456	±0.005	9.10	±0.20
	1.6	1.0254	0.306	±0.009	4.97	±0.16		1.6	0.9835	0.316	±0.009	5.77	±0.21
		2.1035	0.355	±0.006	5.78	±0.13			2.0188	0.362	±0.007	6.67	±0.20
		4.2359	0.402	±0.005	6.50	±0.11			4.0733	0.406	±0.006	7.54	±0.20
		8.1455	0.450	±0.005	7.17	±0.10			7.8511	0.452	±0.008	8.40	±0.22
	1.8	1.4835	0.308	±0.009	4.90	±0.17		1.8	1.4492	0.310	±0.009	5.37	±0.20
		2.8076	0.355	±0.006	5.68	±0.12			2.7385	0.359	±0.007	6.29	±0.19
		5.3157	0.401	±0.005	6.39	±0.11			5.1827	0.404	±0.006	7.13	±0.17
		9.8034	0.449	±0.005	7.06	±0.10			9.5597	0.452	±0.007	7.96	±0.19
	2.0	1.9405	0.306	±0.008	4.79	±0.15		2.0	1.9112	0.308	±0.008	5.13	±0.18
		3.5087	0.354	±0.007	5.57	±0.13			3.4500	0.357	±0.007	6.03	±0.18
		6.3885	0.403	±0.006	6.33	±0.12			6.2756	0.403	±0.005	6.86	±0.16
		11.4483	0.450	±0.005	6.98	±0.10			11.2401	0.452	±0.005	7.67	±0.16

TABLE III. *NPT* MC simulation results for systems 3–6. The reduced temperature is given by $T^*=k_BT/\varepsilon$, the reduced pressure is given by $P^*=P\sigma^3/\varepsilon$, and the reduced energy is given by $E^*=E/N\varepsilon$.

System	T^*	P^*	η	*Error*	$-E^*$	*Error*	System	T^*	P^*	η	*Error*	$-E^*$	*Error*
3	1.2	0.1257	0.328	±0.012	5.78	±0.21	5	1.4	0.4133	0.404	±0.007	13.36	±0.35
		0.7180	0.367	±0.007	6.45	±0.15			2.3741	0.449	±0.005	14.87	±0.32
		2.0974	0.408	±0.006	7.13	±0.13		1.6	0.2593	0.315	±0.015	8.98	±0.47
		4.8272	0.453	±0.005	7.80	±0.11			0.7120	0.356	±0.010	10.13	±0.40
	1.4	0.5748	0.317	±0.010	5.40	±0.19			1.8903	0.402	±0.007	11.58	±0.35
		1.4097	0.361	±0.007	6.15	±0.14			4.4842	0.448	±0.006	13.11	±0.33
		3.1642	0.405	±0.006	6.88	±0.12		1.8	0.8579	0.306	±0.011	7.54	±0.38
		6.4770	0.452	±0.005	7.56	±0.11			1.6498	0.355	±0.009	8.87	±0.37
	1.6	1.0261	0.313	±0.009	5.18	±0.17			3.3105	0.402	±0.007	10.29	±0.34
		2.1027	0.359	±0.007	5.96	±0.15			6.5658	0.448	±0.005	11.73	±0.31
		4.2283	0.405	±0.005	6.70	±0.12		2	1.4198	0.306	±0.009	6.78	±0.31
		8.1153	0.451	±0.005	7.39	±0.11			2.5321	0.354	±0.007	8.02	±0.30
	1.8	1.4789	0.309	±0.008	5.00	±0.16			4.6624	0.402	±0.007	9.36	±0.31
		2.7969	0.356	±0.007	5.79	±0.14			8.5854	0.448	±0.005	10.71	±0.30
		5.2910	0.403	±0.006	6.55	±0.12	6	1.4	0.3080	0.358	±0.010	8.86	±0.31
		9.7472	0.450	±0.005	7.24	±0.11			1.2765	0.399	±0.006	9.91	±0.26
	2	1.9325	0.306	±0.008	4.85	±0.16			3.5146	0.441	±0.006	11.02	±0.25
		3.4917	0.355	±0.007	5.67	±0.14		1.6	0.5306	0.306	±0.014	6.71	±0.35
		6.3529	0.402	±0.005	6.43	±0.12			1.1696	0.354	±0.009	0.79	±0.27
		11.3749	0.451	±0.005	7.13	±0.11			2.5931	0.398	±0.007	8.92	±0.25
4	1.2	0.5921	0.406	±0.006	10.06	±0.25			5.4651	0.442	±0.005	9.99	±0.23
		2.4482	0.449	±0.005	11.22	±0.24		1.8	1.0541	0.303	±0.009	6.12	±0.25
	1.4	0.2353	0.316	±0.013	6.80	±0.31			1.9909	0.352	±0.007	7.21	±0.24
		0.7505	0.362	±0.009	7.83	±0.27			3.8557	0.398	±0.006	8.30	±0.23
		1.9784	0.405	±0.006	8.89	±0.24			7.3631	0.444	±0.005	9.35	±0.22
		4.5180	0.450	±0.005	10.03	±0.23		2	1.5602	0.305	±0.009	5.79	±0.25
	1.6	0.7587	0.309	±0.010	6.03	±0.25			2.7817	0.351	±0.007	6.79	±0.22
		1.5802	0.358	±0.008	7.08	±0.23			5.0741	0.398	±0.006	7.84	±0.22
		3.2709	0.402	±0.007	8.10	±0.23			9.2108	0.445	±0.005	8.88	±0.21
		6.4844	0.448	±0.005	9.17	±0.22		2.2	2.0539	0.304	±0.008	5.52	±0.22
	1.8	1.2596	0.308	±0.009	5.63	±0.23			3.5505	0.351	±0.007	6.50	±0.21
		2.3674	0.356	±0.007	6.62	±0.21			6.2585	0.398	±0.006	7.51	±0.21
		4.4954	0.402	±0.005	7.60	±0.20			11.0161	0.446	±0.005	8.50	±0.20
		8.3632	0.449	±0.005	8.60	±0.20							
	2	1.7466	0.306	±0.009	5.33	±0.22							
		3.1275	0.354	±0.007	6.28	±0.19							
		5.6738	0.401	±0.006	7.24	±0.19							
		10.1765	0.449	±0.005	8.21	±0.19							

$$\frac{A^{\text{assoc}}}{NkT}=\sum_{a=1}^{s}\left(\ln X_a-\frac{X_a}{2}\right)+\frac{s}{2}, \tag{22}$$

where the sum is over all s sites of type a on a molecule, and X_a is the fraction of molecules not bonded at site a,

$$X_a=\frac{1}{1+\sum_{b=1}^{s}\rho X_b\Delta_{a,b}}. \tag{23}$$

The function $\Delta_{a,b}$, which characterizes the association between site a and site b on different molecules, can be written as

$$\Delta_{a,b}=K_{a,b}f_{a,b}g^M(\sigma), \tag{24}$$

where $g^M(\sigma)$ is the contact value of the monomer-monomer radial distribution function, $f_{a,b}=\exp(-\varepsilon_{a,b}^{\text{HB}}/kT)-1$ is the Mayer f function of the a-b site-site bonding interaction $\varepsilon_{a,b}^{\text{HB}}$, and $K_{a,b}$ is the volume available for bonding.[41]

III. MOLECULAR SIMULATIONS

We have performed Monte Carlo (MC) simulations in the isothermal-isobaric (*NPT*) and Gibbs ensembles (GEMC) to determine the *PVT* and phase behavior of several model dipolar associating fluids in order to compare with the theoretical results from the SAFT-VR+D equation for dipolar associating fluids. Molecular simulation studies of associating fluids can be challenging due to the strong association interactions between molecules that can lead to the formation of stable clusters and poor sampling of phase space. As a result, several biasing schemes have been proposed to ensure efficient sampling in MC simulations of associating systems.[42,43] In particular, Tsangaris and de Pablo[43] proposed the bond-bias MC method and compared results from regular GEMC simulations with those using the bond biased move for associating Lennard-Jones monomer fluids with various

TABLE IV. *NPT* MC simulation results for systems 8 and 9. The reduced temperature is given by $T^*=k_BT/\varepsilon$, the reduced pressure is given by $P^*=P\sigma^3/\varepsilon$, and the reduced energy is given by $E^*=E/N\varepsilon$.

System	T^*	P^*	η	*Error*	$-E^*$	*Error*	System	T^*	P^*	η	*Error*	$-E^*$	*Error*
8	1.2	0.7245	0.400	±0.008	9.14	±0.28	9	1.8	1.0610	0.328	±0.010	7.69	±0.29
		2.6045	0.445	±0.005	10.34	±0.24			2.1208	0.369	±0.007	8.70	±0.26
	1.4	0.3146	0.306	±0.013	6.05	±0.31			4.2000	0.410	±0.006	9.76	±0.25
		0.8513	0.355	±0.008	7.08	±0.25			8.0186	0.456	±0.005	10.90	±0.24
		2.1018	0.399	±0.007	8.11	±0.24		2	1.5572	0.319	±0.009	7.07	±0.26
		4.6646	0.445	±0.005	9.22	±0.22			2.8910	0.365	±0.007	8.17	±0.24
	1.6	0.8318	0.306	±0.010	5.52	±0.25			5.3891	0.408	±0.005	9.22	±0.22
		1.6738	0.353	±0.007	6.48	±0.22			9.8429	0.454	±0.005	10.30	±0.22
		3.3861	0.400	±0.006	7.49	±0.21		2.2	2.0440	0.315	±0.008	6.66	±0.24
		6.6221	0.446	±0.006	8.49	±0.22			3.6431	0.361	±0.007	7.74	±0.24
	1.8	1.3273	0.303	±0.009	5.15	±0.21			6.5466	0.407	±0.005	8.81	±0.22
		2.4546	0.353	±0.008	6.11	±0.21			11.6197	0.453	±0.005	9.86	±0.22
		4.6033	0.399	±0.006	7.05	±0.19		2.4	2.5245	0.312	±0.008	6.36	±0.23
		8.4928	0.447	±0.005	8.00	±0.19			4.3831	0.359	±0.006	7.42	±0.22
	2	1.8097	0.302	±0.008	4.93	±0.19			7.6825	0.405	±0.005	8.47	±0.21
		3.2091	0.352	±0.007	5.85	±0.18			13.3622	0.453	±0.005	9.52	±0.21
		5.7752	0.400	±0.006	6.77	±0.18		2.6	3.0004	0.309	±0.008	6.11	±0.22
		10.2988	0.447	±0.005	7.67	±0.18			5.1145	0.357	±0.007	7.17	±0.22
9	1.2	0.2637	0.385	±0.007	8.78	±0.27			8.8029	0.406	±0.005	8.24	±0.20
		2.0708	0.435	±0.006	10.08	±0.25			15.0798	0.452	±0.005	9.22	±0.20
	1.4	0.0165	0.358	±0.013	9.94	±0.39		2.8	3.4731	0.309	±0.007	5.95	±0.22
		0.4825	0.386	±0.007	10.68	±0.28			5.8399	0.356	±0.006	6.98	±0.21
		1.6611	0.419	±0.005	11.64	±0.26			9.9122	0.405	±0.006	8.03	±0.21
		4.1513	0.458	±0.005	12.74	±0.26			16.7788	0.452	±0.005	9.00	±0.20
	1.6	0.5503	0.338	±0.009	8.53	±0.29							
		1.3231	0.377	±0.008	9.52	±0.29							
		2.9646	0.413	±0.006	10.50	±0.25							
		6.1288	0.457	±0.005	11.68	±0.25							

association strengths. They concluded that regular GEMC simulations would fail for systems in which the association energy is ten times or larger than the dispersion energy. In the simulations reported, we study systems with low association energy compared to the dispersion interactions (i.e., $\varepsilon^{HB}<10\varepsilon$) and therefore did not employ any biasing techniques.

As discussed above in the SAFT-VR+D model of dipolar associating fluids, the association sites are situated at a distance r_d from the center of the sphere. Different association sites on the same or different molecules can be bonded with an attractive energy ε^{HB} when the two sites are closer than a distance r_c apart. In the simulations an alternative, but equivalent, potential model based on the distance between two molecules and their respective orientations is used,[41]

$$u(r_{12};\theta_i,\theta_j) = \begin{cases} \varepsilon^{HB}, & \sigma \leqslant r_{ij} < r_{12} \text{ and } |\theta_i| < \theta_c \text{ and } |\pi - |\theta_j|| < \theta_c \\ 0 & \text{otherwise,} \end{cases}$$

where θ_i and θ_j are the angles between the center-to-center vector and the direction vectors on the respective atoms i and j. In Wertheim's theory bonding is limited at each association site to dimers, however, it is possible to get higher order association in the simulations. Recently, Docherty and Galindo[44] have performed extensive simulations to illustrate that the formation of higher order clusters depends on both the size of the association site, the strength of the site-site interaction, and the state condition. In this work the angular cutoff θ_c is set to 27° in order to restrict bonding to dimer formation.[41,45] The cutoff distance r_{12} [Fig. 1(b)] is related to the bonding volume $K_{a,b}$ by

$$K_{a,b} = \sigma^2 \frac{(1-\cos(\theta_c))^2}{4}(r_{12}-\sigma). \tag{25}$$

The reaction field method, which has been used previously to calculate the vapor-liquid phase behavior of systems with long-range dipolar potentials,[26,46] is applied to take into account the long-range dipolar interactions. The reaction field approach replaces the molecules beyond a cutoff distance by a dielectric continuum, the effect of which is taken into account by including a new term into the dipolar potential, viz.,

$$u^{\text{dipole}} = \begin{cases} -(\mu_1\mu_2/r^3)D - 2(\varepsilon_{RF}-1)/2\varepsilon_{RF}+1/\mu_1\mu_2/r_{RF}^3, & r < r_{RF} \\ 0, & r \geqslant r_{RF}, \end{cases} \tag{26}$$

where r_{RF} is the cutoff distance beyond which the pair potential vanishes and ε_{RF} the dielectric constant of the continuum. In our simulations, the value of r_{RF} is set to 2.5σ, and ε_{RF} to ∞.

In the *NPT* ensemble simulations, one cycle consists of three kinds of trial moves: N trial displacements of randomly

TABLE V. GEMC simulation results for the dipolar associating fluids studied (systems 4–9). The density η, number of molecules N, and reduced energy E^* in the coexisting vapor and liquid phases are labeled ν and l, respectively.

System	T^*	η_l	*Error*	η_ν	*Error*	N_l	N_ν	$-E_l^*$	*Error*	$-E_\nu^*$	*Error*
4	0.9	0.464	±0.004	0.001	±0.000	341	171	14.24	±0.19	0.25	±0.19
	1.0	0.446	±0.005	0.004	±0.000	350	162	13.01	±0.23	0.42	±0.12
	1.1	0.417	±0.005	0.004	±0.000	458	54	11.28	±0.21	0.28	±0.15
	1.2	0.381	±0.007	0.012	±0.001	452	60	9.45	±0.22	0.59	±0.19
	1.3	0.346	±0.009	0.030	±0.006	466	46	7.99	±0.24	1.19	±0.37
5	1.0	0.473	±0.004	0.002	±0.000	296	216	19.58	±0.18	14.05	±0.27
	1.1	0.460	±0.005	0.001	±0.000	331	181	18.21	±0.23	0.22	±0.09
	1.2	0.441	±0.005	0.002	±0.000	322	190	16.43	±0.26	0.43	±0.13
	1.3	0.417	±0.007	0.006	±0.000	365	147	14.68	±0.30	0.68	±0.17
	1.4	0.385	±0.007	0.014	±0.001	422	90	12.66	±0.30	1.07	±0.29
6	0.9	0.460	±0.004	0.000	±0.000	368	144	14.96	±0.16	0.11	±0.07
	1.0	0.445	±0.005	0.001	±0.000	375	137	13.99	±0.19	0.11	±0.07
	1.1	0.424	±0.005	0.002	±0.001	503	9	12.61	±0.19	0.21	±0.28
	1.2	0.398	±0.006	0.007	±0.000	365	147	11.03	±0.24	0.49	±0.13
	1.3	0.367	±0.008	0.016	±0.002	334	178	9.59	±0.26	0.85	±0.18
7	0.8	0.445	±0.004	0.000	±0.000	398	114	10.24	±0.13	0.04	±0.03
	0.9	0.423	±0.005	0.002	±0.000	451	61	9.23	±0.13	0.11	±0.06
	1.0	0.399	±0.006	0.004	±0.000	387	125	8.43	±0.15	0.20	±0.07
	1.1	0.372	±0.006	0.010	±0.001	438	74	7.52	±0.14	0.39	±0.13
	1.2	0.339	±0.009	0.022	±0.002	350	162	6.54	±0.18	0.75	±0.13
	1.3	0.288	±0.015	0.045	0.005	331	181	5.48	±0.25	1.35	±0.21
8	0.9	0.461	±0.004	0.002	±0.000	396	116	13.42	±0.19	0.19	±0.09
	1.0	0.435	±0.005	0.003	±0.000	430	82	11.70	±0.19	0.25	±0.11
	1.1	0.400	±0.006	0.007	±0.001	418	94	9.87	±0.23	0.36	±0.13
	1.2	0.364	±0.008	0.018	±0.002	355	157	8.25	±0.25	0.73	±0.17
	1.3	0.318	±0.012	0.046	±0.007	416	96	6.71	±0.27	1.50	±0.32
	1.35	0.278	±0.016	0.072	±0.012	354	158	5.76	±0.31	2.07	±0.40
9	0.9	0.474	±0.005	0.001	±0.000	287	225	16.18	±0.21	8.86	±0.45
	1.0	0.464	±0.003	0.001	±0.000	452	60	16.16	±0.17	0.26	±0.15
	1.1	0.442	±0.005	0.003	±0.003	503	9	14.57	±0.20	0.90	±1.91
	1.2	0.410	±0.006	0.003	±0.000	413	99	12.19	±0.23	0.34	±0.14
	1.3	0.380	±0.007	0.008	±0.001	460	52	10.72	±0.22	0.59	±0.26

chosen molecules, N trial rotations, and one volume change. The maximum extent of each trial move is adjusted to give an individual acceptance probability of 30%–40%. In the GEMC simulations, particle exchanges using the traditional Widom particle insertion method[47] are performed in addition to the three trial moves described above. Each simulation was started from an initial configuration in which 256 molecules are placed on a lattice in the simulation box. An initial simulation of 100 000–500 000 cycles was performed to equilibrate the system, before averaging for between 1 000 000 and 4 000 000 cycles. The thermodynamic properties of the system were obtained as ensemble averages and the errors estimated by determining the standard deviation.

Before studying the dipolar associating fluids of interest in this work, to check the accuracy of our simulation code, we performed *NPT* simulations for several hard associating fluids and obtained good agreement with the results of Jackson *et al.*[48] for fluids with one and two association sites and Slovak and Nezbeda[49] and Ghonasgi and Chapman[50] for fluids with four association sites.

IV. RESULTS AND DISCUSSION

We have applied the SAFT-VR+D approach to study the *PVT* and phase behavior of several dipolar associating fluids. In order to validate and test the predictive ability of the SAFT-VR+D EOS for associating fluids before application to real dipolar associating fluids, such as water and alcohols, *NPT* and Gibbs ensemble Monte Carlo simulations have been performed for several dipolar associating fluids with one association site (system 1), two association sites (system 2), and four association sites with different strengths of the association energy (systems 3–5), association volume (systems 6 and 7), and dipole moment (systems 8 and 9). The details of each system studied are given in Table I. The results of the *NPT* simulations are reported in Tables II–IV and those of the GEMC simulations are given in Table V.

In Fig. 2 we present the *PVT* behavior for dipolar associating fluids with one association site [system 1, Fig. 2(a)] and two association sites [system 2, Fig. 2(b)], with all other parameters the same (i.e., $\mu^{*2}=1$, $\lambda=1.5$, $r_{12}^*=1.05$, $\varepsilon^*=1$, and $\varepsilon^{HB^*}=5$). From Fig. 2, we find that the fluid with two

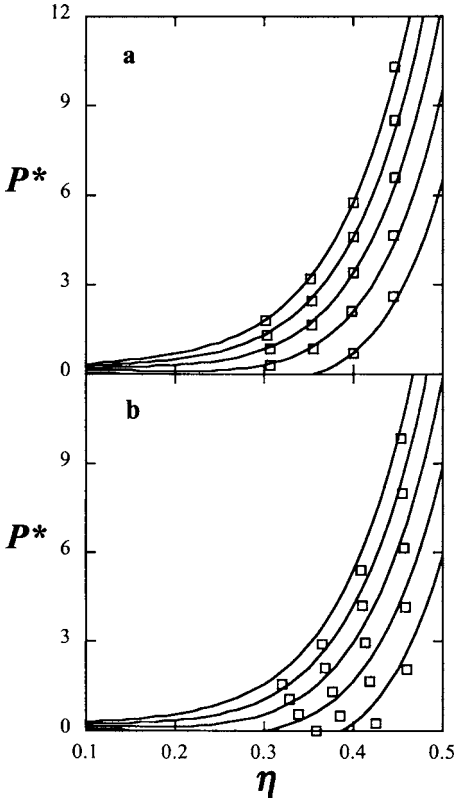

FIG. 2. Comparison of predictions from the SAFT-VR+D approach and simulation data for isotherms of dipolar square-well associating monomer fluids with (a) one association site and (b) two association sites, with $\varepsilon^*=1.0$, $\lambda=1.5$, $\sigma^*=1.0$, $\mu^{*2}=1.0$, $r_{12}^*=1.05$, and $\varepsilon^{HB^*}=5.0$ at $T^*=1.2$, 1.4, 1.6, 1.8, and 2.0 (from bottom to top). The solid lines represent predictions from the SAFT-VR+D equation and the symbols *NPT* Monte Carlo simulation data.

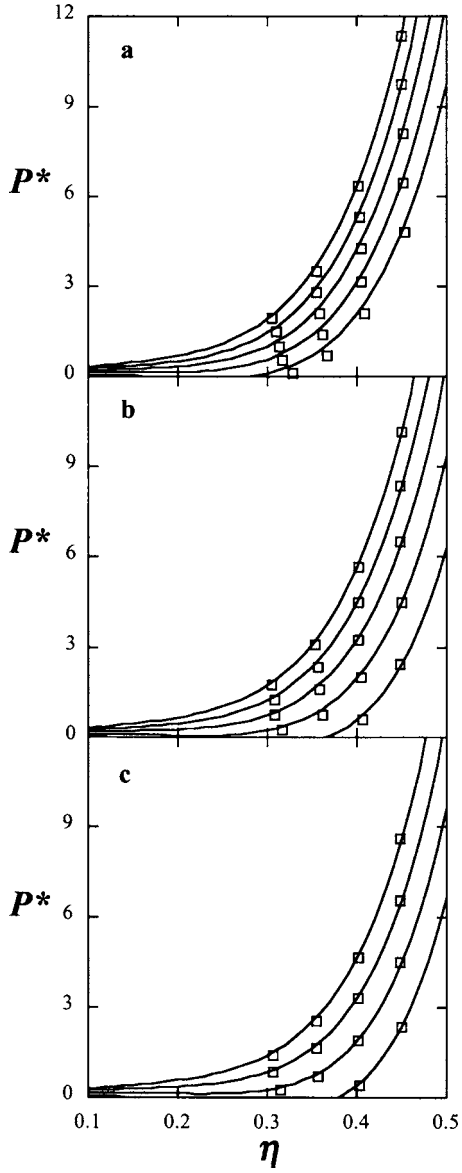

FIG. 3. Comparison of predictions from the SAFT-VR+D approach and simulation data for isotherms of dipolar square-well associating monomer fluids with four association sites with $\varepsilon^*=1.0$, $\lambda=1.5$, $\sigma^*=1.0$, $\mu^{*2}=1.0$, $r_{12}^*=1.05$, and (a) $\varepsilon^{HB^*}=2.0$ at $T^*=1.2$, 1.4, 1.6, 1.8, and 2.0 (from bottom to top), (b) $\varepsilon^{HB^*}=5.0$ at $T^*=1.2$, 1.4, 1.6, 1.8, and 2.0 (from bottom to top), and (c) $\varepsilon^{HB^*}=7.0$ at $T^*=1.4$, 1.6, 1.8, and 2.0 (from bottom to top). The solid lines represent predictions from the SAFT-VR+D equation and the symbols *NPT* Monte Carlo simulation data.

association sites exhibits higher densities at a given temperature and pressure than the fluid with one association site, which would be expected given the greater cohesion energy between the molecules, and that good agreement is obtained between the simulation results and theoretical predictions for each of the systems studied. It is important to note that the theoretical curves contain no adjustable parameters and are the SAFT-VR+D predictions for the same system as that simulated; hence, this is a direct test of the SAFT-VR+D theory for dipolar associating fluids. In Fig. 3 we present the *PVT* behavior for dipolar associating fluids with four association sites and different association energies (systems 3–5). For each system studied the remaining SAFT-VR+D parameters are the same: $\mu^{*2}=1$, $\lambda=1.5$, $r_{12}^*=1.05$, and $\varepsilon^*=1$. From Fig. 3, we find that the fluids with higher association energy exhibit higher densities at a given temperature and pressure than those with lower association energy. Similarly, when compared with the *PVT* behavior for dipolar associating fluids with one and two association sites (system 1 and 2), the fluid with four association sites and all other parameters the same (i.e., system 4) exhibits higher densities at a given temperature and pressure. Again, good agreement is observed between the simulation results and theoretical predictions for each of the systems studied over a wide range of temperatures and pressures.

We have also determined the fluid phase diagram for systems 4 and 5 in order to further test the SAFT-VR+D approach. From the results presented in Fig. 4, and as would be expected, we find that the fluid with the higher association energy ($\varepsilon^{HB^*}=7$, system 5) has a higher critical temperature and wider phase envelope than the fluid with a lower association energy ($\varepsilon^{HB^*}=5$, system 4). Additionally good agreement is obtained between the simulation results and theoretical predictions for both systems studied. From these results, we can conclude that the SAFT-VR+D approach provides a good description of the thermodynamic properties of dipolar associating fluids with one, two, or four association sites as a function of association energy (i.e., from $\varepsilon^{HB^*}=2$ to $\varepsilon^{HB^*}=7$).

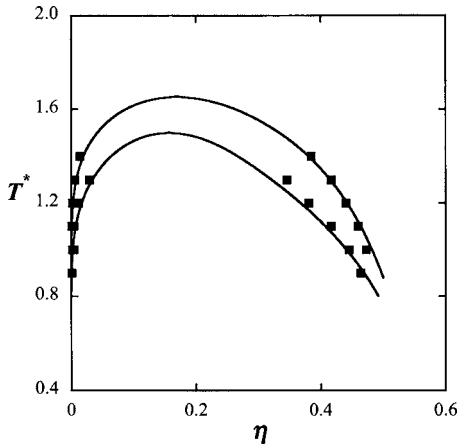

FIG. 4. Comparison of predictions from the SAFT-VR+D approach and simulation data for coexisting densities of dipolar square-well associating monomer fluids with four association sites (a) system 4: $\mu^{*2}=1$, $\lambda=1.5$, $r_{12}^{*}=1.05$, $\varepsilon^{*}=1$, and $\varepsilon^{HB^{*}}=5$ (bottom); (b) system 5: $\mu^{*2}=1$, $\lambda=1.5$, $r_{12}^{*}=1.05$, $\varepsilon^{*}=1$, and $\varepsilon^{HB^{*}}=7$ (top). The symbols represent the GEMC simulation data and the solid lines predictions from the SAFT-VR+D equation.

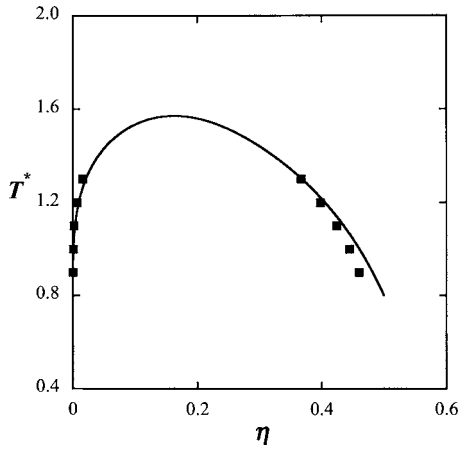

FIG. 6. Comparison of predictions from the SAFT-VR+D approach and simulation data for the coexisting densities of dipolar square-well associating monomer fluids with four association sites and $\mu^{*2}=1$, $\lambda=1.5$, $r_{12}^{*}=1.1$, $\varepsilon^{*}=1$, and $\varepsilon^{HB^{*}}=5$ (system 6). The circles represent the GEMC simulation data and the solid lines predictions from the SAFT-VR+D equation.

Since a square-well potential is applied to mimic the hydrogen bonding interaction, the volume or range of the association interaction r_{12}^{*} plays an important role in the thermodynamic properties of dipolar associating fluids. In order to examine the effect of r_{12}^{*} on the phase behavior of dipolar associating fluids and further test the SAFT-VR+D approach, we have studied the *PVT* behavior of a dipolar square-well associating fluid with $\lambda=1.5$, $\sigma^{*}=1.0$, $\varepsilon^{*}=1.0$, $\mu^{*2}=1.0$, $\varepsilon^{HB^{*}}=5.0$, and $r_{12}^{*}=1.1$ (system 6) to compare to the results for system 4, for which $r_{12}^{*}=1.05$ (with all other parameters the same). The results are presented in Fig. 5 and when compared to those for system 4 [Fig. 3(b)] we note that as r_{12}^{*} increases the density of the system decreases at a given pressure and temperature, which reflects weaker intermolecular interactions between the molecules for smaller values of r_{12}^{*}. Good agreement is again observed between the theoretical predictions and the simulation data. We have also studied the phase diagram for system 6, the results of which are presented in Fig. 6. From a comparison of Figs. 6 and 4 (bottom line, system 4) we see that as the cutoff distance is increased the critical temperature of the dipolar associating fluid increases, due to the increase in the attractive association interaction. Good agreement is seen between the theoretical phase diagram from the SAFT-VR+D approach and the GEMC simulation data, though we note slight deviations are observed at low temperature ($T^{*}<1.1$). The observed deviations could be due to the association interactions prohibiting efficient sampling of phase space or a shortcoming in the theory. We note that good agreement is obtained at low temperatures for system 4, which has a shorter association range and therefore overall weaker association interactions. Furthermore, if we compare the results for system 6 with those for system 7 (Fig. 7), which has a lower association energy ($\varepsilon^{HB^{*}}=3.0$) with the other parameters the same, we again see that the SAFT-VR+D approach provides good agreement with the simulation data at low temperatures. We

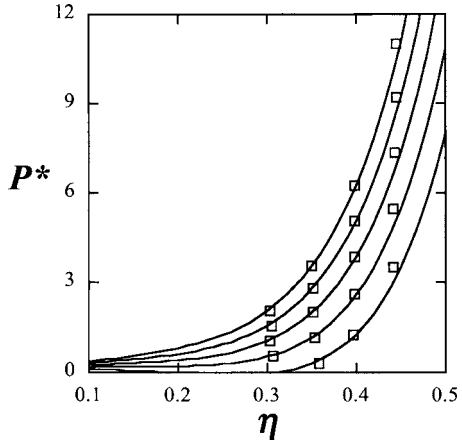

FIG. 5. Comparison of predictions from the SAFT-VR+D approach and simulation data for isotherms of dipolar square-well associating monomer fluids with four association sites for system 6: $\mu^{*2}=1$, $\lambda=1.5$, $r_{12}^{*}=1.1$, $\varepsilon^{*}=1$, and $\varepsilon^{HB^{*}}=5$ at $T^{*}=1.2$, 1.4, 1.6, 1.8, 2.0 (from bottom to top). The solid lines represent predictions from the SAFT-VR+D equation and the symbols the *NPT*-MC simulation data.

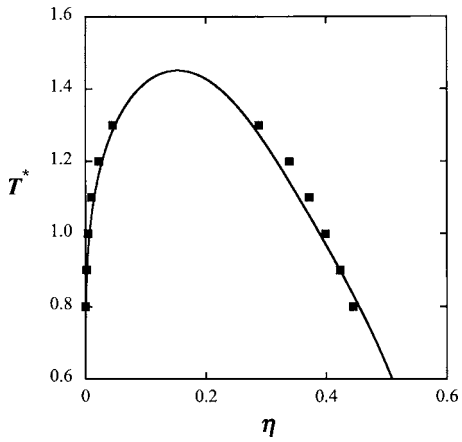

FIG. 7. Comparison of predictions from the SAFT-VR+D approach and simulation data for the coexisting densities of dipolar square-well associating monomer fluids with four association sites and $\mu^{*2}=1$, $\lambda=1.5$, $r_{12}^{*}=1.1$, $\varepsilon^{*}=1$, and $\varepsilon^{HB^{*}}=3$ (system 7). The circles represent the GEMC simulation data and the solid lines predictions from the SAFT-VR+D equation.

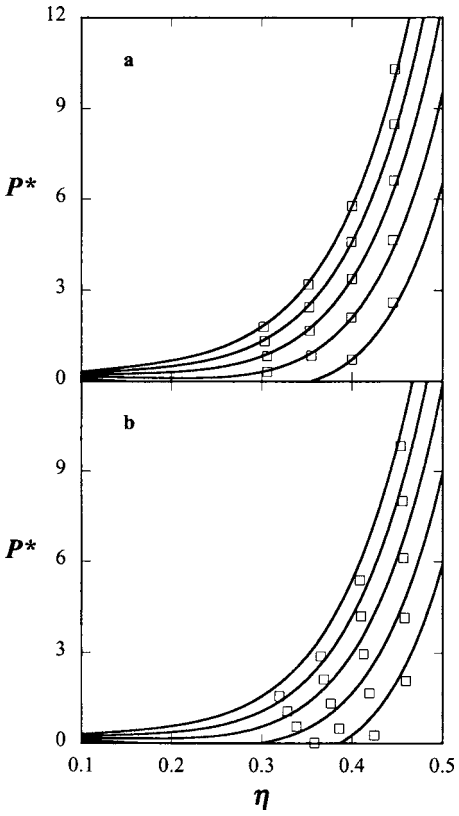

FIG. 8. Comparison of predictions from the SAFT-VR+D approach and simulation data for isotherms of dipolar square-well associating monomer fluids with four association sites $\lambda=1.5$, $r_{12}^{*}=1.05$, $\varepsilon^{*}=1$, and $\varepsilon^{HB^{*}}=5$ at $T^{*}=1.2$, 1.4, 1.6, 1.8, and 2.0 (from bottom to top) and (a) $\mu^{*2}=0.5$ and (b) $\mu^{*2}=2$. The solid lines represent predictions from the SAFT-VR+D equation and the symbols the *NPT* MC simulation data.

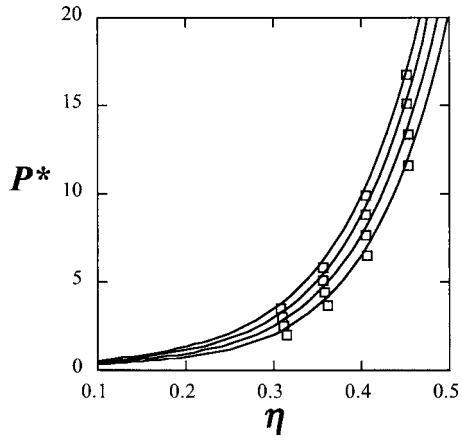

FIG. 9. Comparison of predictions from the SAFT-VR+D approach and simulation data for isotherms of dipolar square-well associating monomer fluids with four association sites and $\mu^{*2}=2$, $\lambda=1.5$, $r_{12}^{*}=1.05$, $\varepsilon^{*}=1$, and $\varepsilon^{HB^{*}}=5$ (system 9) at $T^{*}=2.2$, 2.4, 2.6, 2.8 (from bottom to top). The solid lines represent predictions from the SAFT-VR+D equation and the cycles the *NPT* MC simulation data.

therefore conjecture, since the underprediction is only observed in the liquid density at low temperatures for system 6 in which the association energy is at its strongest, that the association interactions are preventing efficient sampling of the system.

We now turn to the effect of the strength of the dipole moment on the *PVT* and phase behavior of dipolar associating fluids. In Fig. 8 we present the *PVT* behavior of dipolar associating fluids with four association sites with different dipole moments, namely, systems 8 and 9 for which $\mu^{*2}=0.5$ and $\mu^{*2}=2$, respectively, with all other parameters the same ($\lambda=1.5$, $r_{12}^{*}=1.05$, $\varepsilon^{*}=1$, and $\varepsilon^{HB^{*}}=5$). From Fig. 8(a), we see excellent agreement is observed between the predictions from the SAFT-VR+D approach and simulation data. However, the SAFT-VR+D approach slightly underpredicts the density at a given temperature and pressure for system 9, as shown in Fig. 8(b). In Fig. 9, isotherms for system 9 are presented at higher temperatures ($T^{*}=2.2,2.4,2.6,2.8$) and we note that better agreement between the simulation results and theoretical predictions are observed. We have also studied the phase equilibria of systems 8 and 9 as shown in Fig. 10. For system 8, we obtain excellent agreement between the simulation results and theoretical predictions from the SAFT-VR+D approach; however, we see a slight deviation between the theoretical predictions and simulation data for system 9 with the higher dipole moment, which is consistent with earlier work.[21]

Having seen that SAFT-VR+D equation can accurately describe the fluid phase behavior of dipolar square-well associating fluids with one, two, and four association sites, we now turn to the study of real fluids, and specifically water. The experimental dipole moment for water is used in the calculations and the remaining parameters are determined by fitting to experimental vapor pressure and saturated liquid density data.[51] These are reported in Table VI along with those for the original SAFT-VR approach.[52] We compare the results obtained with those from the original SAFT-VR equation in Fig. 11. From the figure, we can see that the predicted critical temperature from the SAFT-VR+D approach is slightly lower than that of the SAFT-VR EOS though both methods overpredict the critical point due to the analytic nature of the equations of state.[24] Although from a visual inspection the agreement with experimental data from the two approaches is comparable, the SAFT-VR+D equation

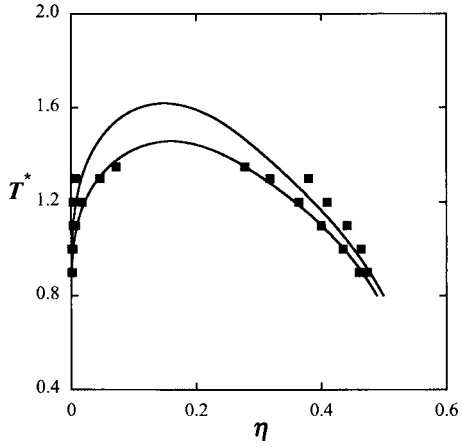

FIG. 10. Comparison of predictions from the SAFT-VR+D approach and simulation data for coexisting densities of dipolar square-well associating monomer fluids with four association sites for (a) system 8: $\mu^{*2}=0.5$, $\lambda=1.5$, $r_{12}^{*}=1.05$, $\varepsilon^{*}=1$, and $\varepsilon^{HB^{*}}=5$ and (b) system 9: $\mu^{*2}=2$, $\lambda=1.5$, $r_{12}^{*}=1.05$, $\varepsilon^{*}=1$, and $\varepsilon^{HB^{*}}=5$. The symbols represent the GEMC simulation data and the solid lines predictions from the SAFT-VR+D equation.

TABLE VI. Parameters used in the SAFT-VR+D and SAFT-VR approaches for water. ε/k is the depth in Kelvin and λ the range of the square-well potential potential, σ is the diameter in angstrom, m the number of segments, ε^{HB}/k the association energy in Kelvin, K the volume of the association interaction, and μ the dipole moment in Debye.

Water	ε/k (K)	σ (Å)	λ	m	ε^{HB}/k (K)	K (Å^3)	μ (D)
SAFT-VR+D	389.87	3.061	1.48	1	900.55	1.467	1.84
SAFT-VR[a]	253.3	3.036	1.8	1	1366.0	1.028	···

[a]Reference 52.

provides a slightly more accurate correlation of both the vapor pressure and saturated liquid density of water than the SAFT-VR equation when the absolute average deviations (AADs) are calculated: the AAD over the whole phase diagram is 0.92% for the vapor pressures and 2.87% for saturated liquid densities for the SAFT-VR+D approach, compared with 1.18% and 3.06%, respectively, for the SAFT-VR equation. We also note from Fig. 11 that both the SAFT-VR and SAFT-VR+D equations do not capture the experimentally observed density maximum of water at lower temperature. We find that in order to capture this behavior a temperature-dependent segment diameter is needed; a similar result is obtained using the SAFT1 equation,[53] which uses temperature-dependent parameters to describe the water phase diagram.

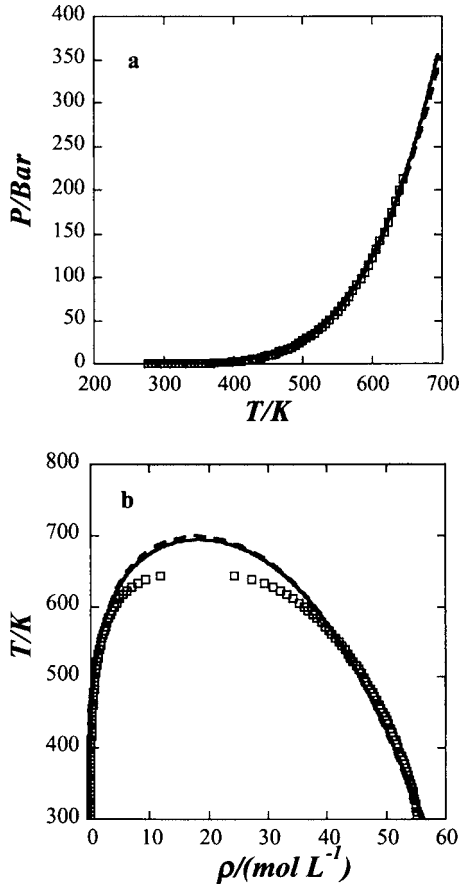

FIG. 11. Experimental vapor pressures (a) and vapor-liquid coexisting densities (b) for water compared with theoretical predictions. The results obtained from the SAFT-VR EOS are represented as dashed lines and those from the SAFT-VR+D equation as solid lines. The squares represent experimental data.

V. CONCLUSION

The SAFT-VR+D approach for dipolar associating fluids has been presented and *NPT* MC and GEMC simulations performed to obtain simulation data with which to compare and validate the SAFT-VR+D approach for dipolar associating fluids. The theoretical predictions are found to be in good agreement with the simulation data for dipolar associating fluids with one, two, and four association sites. The effect of the range of association energy and association volume on the thermodynamic properties and phase behavior has also been studied and good agreement obtained between the theoretical predictions and simulation data, though slight deviations are seen for the saturated liquid densities at low temperature/pressure for the strongest association system studied. This is conjectured to be due to poor sampling in the GEMC simulations due to the formation of clusters of associating molecules, rather than a deficiency of the theory. The comparison between the theoretical predictions and simulation data illustrates that the SAFT-VR+D approach can accurately describe the thermodynamic properties of dipolar associating fluids. Additionally, we have applied the SAFT-VR+D approach to water. Although the improvement seen in the description of the fluid phase diagram is minimal compared to the original SAFT-VR approach, the dipolar model for water allows us to explicitly study the effect of the dipolar interactions on solvent properties. Hence it will be especially useful for modeling electrolyte solutions[54] and water-nonpolar mixtures in which the asymmetry in solute-solvent and solvent-solvent interactions drives the nonideality in such systems.

ACKNOWLEDGMENTS

We gratefully acknowledge financial support from the National Science Foundation under Grant No. CTS-0452688. The authors would also like to thank Amparo Galindo for useful discussions.

[1] S. Gupta and J. D. Olson, Ind. Eng. Chem. Res. **42**, 6359 (2003).
[2] G. M. Kontogeorgis, E. C. Voutsas, I. V. Yakoumis, and D. P. Tassios, Ind. Eng. Chem. Res. **35**, 4310 (1996).
[3] G. M. Kontogeorgis, I. V. Yakoumis, H. Meijer, E. Hendriks, and T. Moorwood, Fluid Phase Equilib. **160**, 201 (1999); E. C. Voutsas, I. V. Yakoumis, and D. P. Tassios, *ibid.* **160**, 151 (1999).
[4] G. K. Folas, G. M. Kontogeorgis, M. L. Michelsen, and E. H. Stenby, Ind. Eng. Chem. Res. **45**, 1516 (2006).
[5] G. D. Ikonomou and M. D. Donohue, Fluid Phase Equilib. **33**, 61 (1987); AIChE J. **32**, 1716 (1986).
[6] G. D. Ikonomou and M. D. Donohue, Fluid Phase Equilib. **39**, 129 (1988).
[7] W. G. Chapman, K. E. Gubbins, G. Jackson, and M. Radosz, Fluid Phase Equilib. **52**, 31 (1989); Ind. Eng. Chem. Res. **29**, 1709 (1990).

[8] M. S. Wertheim, J. Stat. Phys. **35**, 19 (1984); **35**, 35 (1984); **42**, 459 (1986); **42**, 477 (1986).
[9] E. A. Muller and K. E. Gubbins, in *Equations of State for Fluids and Fluid Mixtures*, edited by J. V. Sengers, R. F. Kayser, C. J. Peters, and H. J. J. White (Elsevier, Amsterdam, 2000), Vol. I, p. 435; I. G. Economou, Ind. Eng. Chem. Res. **41**, 953 (2002).
[10] K. E. Gubbins and C. G. Gray, Mol. Phys. **23**, 187 (1972).
[11] G. Stell, J. C. Rasaiah, and H. Narang, Mol. Phys. **23**, 393 (1972).
[12] E. A. Muller and K. E. Gubbins, Ind. Eng. Chem. Res. **34**, 3662 (1995).
[13] T. Kraska and K. E. Gubbins, Ind. Eng. Chem. Res. **35**, 4727 (1996); **35**, 4738 (1996).
[14] I. Nezbeda and U. Weingerl, Mol. Phys. **99**, 1595 (2001).
[15] Z. P. Liu, Y. G. Li, and K. Y. Chan, Ind. Eng. Chem. Res. **40**, 973 (2001).
[16] P. K. Jog and W. G. Chapman, Mol. Phys. **97**, 307 (1999); P. K. Jog, S. G. Sauer, J. Blaesing, and W. G. Chapman, Ind. Eng. Chem. Res. **40**, 4641 (2001).
[17] F. Tumakaka and G. Sadowski, Fluid Phase Equilib. **217**, 233 (2004).
[18] A. Dominik, W. G. Chapman, M. Kleiner, and G. Sadowski, Ind. Eng. Chem. Res. **44**, 6928 (2005).
[19] B. Saager and J. Fischer, Fluid Phase Equilib. **72**, 67 (1992); B. Saager, J. Fischer, and M. Neumann, Mol. Simul. **6**, 27 (1991).
[20] J. Gross and J. Vrabec, AIChE J. **52**, 1194 (2006).
[21] H. Zhao and C. McCabe, J. Chem. Phys. **125**, 4504 (2006).
[22] A. Gil-Villegas, A. Galindo, P. J. Whitehead, S. J. Mills, G. Jackson, and A. N. Burgess, J. Chem. Phys. **106**, 4168 (1997).
[23] C. McCabe and G. Jackson, Phys. Chem. Chem. Phys. **1**, 2057 (1999); C. McCabe, A. Galindo, M. N. Garcia-Lisbona, and G. Jackson, Ind. Eng. Chem. Res. **40**, 3835 (2001).
[24] C. McCabe and S. B. Kiselev, Fluid Phase Equilib. **219**, 3 (2004); C. MaCabe and S. B. Kiselev, Ind. Eng. Chem. Res. **43**, 2839 (2004).
[25] C. McCabe, A. Galindo, A. Gil-Villegas, and G. Jackson, Int. J. Thermophys. **19**, 1511 (1998); C. McCabe, A. Gil-Villegas, and G. Jackson, J. Phys. Chem. B **102**, 4183 (1998); A. Galindo, L. J. Florusse, and C. J. Peters, Fluid Phase Equilib. **160**, 123 (1999); E. J. M. Filipe, E. de Azevedo, L. F. G. Martins, V. A. M. Soares, J. C. G. Calado, C. McCabe, and G. Jackson, J. Phys. Chem. B **104**, 1315 (2000); E. J. M. Filipe, L. F. G. Martins, J. C. G. Calado, C. McCabe, and G. Jackson, *ibid.* **104**, 1322 (2000); E. J. M. Filipe, L. M. B. Dias, J. C. G. Calado, C. McCabe, and G. Jackson, Phys. Chem. Chem. Phys. **4**, 1618 (2002); L. M. B. Dias, E. J. M. Filipe, C. McCabe, and J. C. G. Calado, J. Phys. Chem. B **108**, 7377 (2004); L. X. Sun, H. G. Zhao, S. B. Kiselev, and C. McCabe, *ibid.* **109**, 9047 (2005); H. G. Zhao, P. Morgado, C. McCabe, and A. Gil Villegas, *ibid.* **110**, 24083 (2006); L. Sun, H. Zhao, and C. McCabe, AIChE J. **53**, 720 (2007).
[26] L. X. Sun, H. G. Zhao, S. B. Kiselev, and C. McCabe, Fluid Phase Equilib. **228**, 275 (2005).
[27] C. McCabe, A. Galindo, A. Gil-Villegas, and G. Jackson, J. Phys. Chem. B **102**, 8060 (1998); R. P. Bonifacio, E. J. M. Filipe, C. McCabe, M. F. C. Gomes, and A. A. H. Padua, Mol. Phys. **100**, 2547 (2002); P. Morgado, C. McCabe, and E. J. M. Filipe, Fluid Phase Equilib. **228**, 389 (2005); P. Morgado, H. Zhao, F. J. Blas, C. McCabe, L. P. N. Rebelo, and E. J. M. Filipe, J. Phys. Chem. B **111**, 2856 (2005).
[28] F. J. Blas and A. Galindo, Fluid Phase Equilib. **194–197**, 501 (2002).
[29] L. M. B. Dias, R. P. Bonifacio, E. J. M. Filipe, J. C. G. Calado, C. McCabe, and G. Jackson, Fluid Phase Equilib. **205**, 163 (2003).
[30] L. M. B. Dias, E. J. M. Filipe, C. McCabe, T. Cordeiro, and J. C. G. Calado, J. Phys. Chem. B **111**, 5284 (2007).
[31] C. McCabe, A. Galindo, and P. T. Cummings, J. Phys. Chem. B **107**, 12307 (2003); A. Valtz, A. Chapoy, C. Coquelet, P. Paricaud, and D. Richon, Fluid Phase Equilib. **226**, 333 (2004).
[32] A. Galindo, A. Gil-Villegas, P. J. Whitehead, G. Jackson, and A. N. Burgess, J. Phys. Chem. B **102**, 7632 (1998).
[33] A. Galindo and F. J. Blas, J. Phys. Chem. B **106**, 4503 (2002); C. M. Colina, A. Galindo, F. J. Blas, and K. E. Gubbins, Fluid Phase Equilib. **222**, 77 (2004); C. M. Colina and K. E. Gubbins, J. Phys. Chem. B **109**, 2899 (2005).
[34] J. S. Hoye, J. L. Lebowitz, and G. Stell, J. Chem. Phys. **61**, 3253 (1974); G. Stell and S. F. Sun, J. Chem. Phys. **63**, 5333 (1975).
[35] J. A. Barker and D. Henderson, J. Chem. Phys. **47**, 2856 (1967); **47**, 4714 (1967).
[36] N. F. Carnahan and K. E. Starling, J. Chem. Phys. **51**, 635 (1969).
[37] A. Gil-Villegas, A. Galindo, P. J. Whitehead, S. J. Mills, G. Jackson, and A. N. Burgess, J. Chem. Phys. **106**, 4168 (1997).
[38] J. A. Barker and D. Henderson, Rev. Mod. Phys. **48**, 587 (1975).
[39] M. S. Wertheim, J. Chem. Phys. **55**, 4291 (1971).
[40] W. G. Chapman, G. Jackson, and K. E. Gubbins, Mol. Phys. **65**, 1057 (1988).
[41] G. Jackson, W. G. Chapman, and K. E. Gubbins, Mol. Phys. **65**, 1 (1988).
[42] D. P. Visco and D. A. Kofke, J. Chem. Phys. **110**, 5493 (1999); **114**, 8752 (2001); B. Chen and J. I. Siepmann, J. Phys. Chem. B **104**, 8725 (2000); **105**, 11275 (2001).
[43] D. M. Tsangaris and J. J. de Pablo, J. Chem. Phys. **101**, 1477 (1994).
[44] H. Docherty and A. Galindo, Mol. Phys. **104**, 3551 (2006).
[45] J. K. Singh and D. A. Kofke, J. Chem. Phys. **121**, 9574 (2004).
[46] J. A. Barker and R. O. Watts, Mol. Phys. **26**, 789 (1973).
[47] B. Widom, J. Chem. Phys. **39**, 2808 (1963).
[48] G. Jackson, W. G. Chapman, and K. E. Gubbins, Int. J. Thermophys. **9**, 769 (1988).
[49] J. Slovak and I. Nezbeda, Mol. Phys. **101**, 789 (2003).
[50] D. Ghonasgi and W. G. Chapman, Mol. Phys. **79**, 291 (1993).
[51] CRC, *Handbook of Chemistry and Physics* (CRC, Cleveland, OH, 1981).
[52] A. Galindo, A. Gil-Villegas, G. Jackson, and A. N. Burgess, J. Phys. Chem. B **103**, 10272 (1999).
[53] H. Adidharma and M. Radosz, Ind. Eng. Chem. Res. **37**, 4453 (1998); S. P. Tan, H. Adidharma, and M. Radosz, *ibid.* **44**, 4442 (2005).
[54] H. G. Zhao and C. McCabe, J. Chem. Phys. **126**, 4503 (2007).